

Research Article

Facile Synthesis of Ethyl Acetate over $\text{ZrO}_2\cdot\text{TiO}_2$ Mixed Oxide Supported Vanadium Boosted Phosphomolybdic Acid Catalyst at Room Temperature

Balaga Viswanadham 

Chemistry Division, Department of Basic Sciences and Humanities, GMR Institute of Technology (Affiliated to JNTU-GV), GMR Nagar, Rajam 532127, Andhra Pradesh, India

Correspondence should be addressed to Balaga Viswanadham; viswanadham.b@gmrit.edu.in

Received 28 July 2023; Revised 5 November 2023; Accepted 24 November 2023; Published 6 December 2023

Academic Editor: Ahmad M. Mohammad

Copyright © 2023 Balaga Viswanadham. This is an open access article distributed under the Creative Commons Attribution License, which permits unrestricted use, distribution, and reproduction in any medium, provided the original work is properly cited.

Initially, mixed oxide of $\text{ZrO}_2\cdot\text{TiO}_2$ support was synthesized by the sol-gel method, and then after vanadium was incorporated, phosphomolybdic acid (VPMA) was synthesized by the hydrothermal method. VPMA supported on $\text{ZrO}_2\cdot\text{TiO}_2$ support of various VPMA loadings that were synthesized by the impregnation method. The structure, surface area, acidity, and morphology of the materials were analysed by X-ray diffraction, BET surface area, ammonia TPD studies, and SEM analysis, respectively. The XRD result shows crystallites of zirconia, titania, and Keggin ion of VPMA catalysts, and also, below 20 wt% of VPMA loading, crystallites of Keggin ion are not observed. BET surface area analysis reveals that increase of VPMA loading, surface area was sharply declined at higher loadings. Ammonia TPD analysis finds that acidity is inclined with VPMA loadings. SEM studies reveal that bulk formation of the active phase is observed at higher loadings. Esterification of acetic acid was tested over VPMA/ $\text{ZrO}_2\cdot\text{TiO}_2$ catalyst that exhibited higher activity during reaction than pure VPMA catalyst. These findings were well correlated with surface area and acidity loadings.

1. Introduction

Polyoxometalates (POMs) are well-known solid acid catalysts because of their tunable acid and redox properties of materials for various kinds of reactions [1, 2]. In recent years, POMs gained more attention due to industrial applications of different acid and oxidation reactions [3–15]. POMs are strong Brønsted acid materials. However, their major limitation is their low surface area, which has an impact on their catalytic property during reaction. The limitation of lower surface area of pure POMs can be minimized by while promoting active POMs on support of single or mixed oxide results higher surface area as well as acidity can boost the catalytic performance [5–9]. Vanadium containing POMs were studied in various reactions such as dehydration, condensation, and other reactions [3, 16, 17]. It is also important that support makes the active phase more stable,

as well as more number of active sites are important for higher catalytic activity during the reaction. In recent times, $\text{ZrO}_2\cdot\text{TiO}_2$ mixed oxide was used as support in various reactions [18–20]. In the view of several organic conversions studied over V modified phosphomolybdic acid (VPMA) catalyst, we studied esterification of acetic acid over VPMA supported on mixed $\text{ZrO}_2\cdot\text{TiO}_2$ catalyst at room temperature.

The catalytic esterification of acetic acid to alkyl acetate has a marked importance in both applied and basic research which is because of the huge applications of ester in industrial and academic usages. Ethyl acetate or alkyl acetate is synthesized by using mineral acid such as sulphuric or phosphoric acid, which is a corrosive process due to reactors that were damaged during the course of reaction. In addition, using larger quantities of sulfuric acid as a catalyst causes coke to form during the production of ethyl acetate. Another

disadvantage of using sulfuric acid as a catalyst is that it produces acetaldehyde. Consequently, acetaldehyde's competition with the other reactants reduces the ester yields [21–23]. However, sulphuric acid materials are corrosive, and isolation of the product is not easy and eco-friendly. Therefore, the development of a catalyst is eco-friendly and not corrosive and easy isolation of the product is challenging for researchers and scientists.

In this present work, studied esterification of acetic acid over zirconia and titania mixed oxide supported vanadium-modified phosphomolybdic acid catalysts. The aim of this study is the effect of VPMA on $ZrO_2.TiO_2$ support during the reaction. We also studied the various reaction parameters such as amount of catalyst, mole ratio of reactants, time on stream, and different alcohols to optimize the higher activity towards the product of ethyl acetate. The purpose of the present study is to estimate the acidity of VPMA on $ZrO_2.TiO_2$ and mark a relation between catalytic performance and acidity.

2. Materials and Methods

2.1. Materials. MOO_3 , V_2O_5 , zirconium (IV) isopropoxide, and titanium (IV) isopropoxide were procured from Aldrich, and H_3PO_4 was supplied from SD Fine Ltd.

2.2. Methods. $ZrO_2.TiO_2$ mixed oxide support was synthesised by using zirconium (IV) isopropoxide and titanium (IV) isopropoxide as a precursor. About 1 : 1 mole ratio of zirconium (IV) isopropoxide and titanium (IV) isopropoxide is initially mixed to get a homogeneous mixture and then hydrolysis by slow addition of 20 ml of distilled water results into a white precipitate. This is washed with distilled water, dried, then calcined at 300°C for 3 h, and labelled as $ZrO_2.TiO_2$ support. Vanadium-substituted PMA (VPMA = $H_4PMo_{11}VO_{40}$) was synthesized by the hydrothermal method according to the literature method [3]. The various VPMA loadings from 10 to 50 wt% VPMA supported on $ZrO_2.TiO_2$ by the impregnation method and thereafter calcined at 200°C for 3 h.

2.3. Characterization Techniques. X-ray powder diffraction patterns of the samples were obtained with a model: D8 diffractometer (Advance, Bruker, Germany) using $Cu K\alpha$ radiation (1.5406 Å) at 40 kV and 30 mA. The measurements were recorded in steps of 0.0450 with a count time of 0.5 s in

the range of 2–65°. Temperature-programmed desorption (TPD) studies of NH_3 were conducted on the Auto Chem 2910 (micromeritics, USA) instrument. The ammonia concentration in the effluent stream was monitored with the thermal conductivity detector, and the area under the peak was integrated using the software GRAMS/32 to determine the amount of desorbed ammonia. BET surface area analysis was performed on the Auto Chem 2910 analyzer. Pyridine-adsorbed FT-IR spectra of samples were analyzed by using the FT-IR Nicolet 670 spectrometer with the KBr disc method at room temperature. The SEM analyses of samples were recorded on S-4800 microscopy.

2.4. Catalytic Esterification. The catalysts were tested for esterification of acetic acid with ethanol in a 50 mL round bottom flask at room temperature. In the experiment (Scheme 1), 10 mmol of acetic acid, 20 mmol of ethanol, and 0.1 g of the catalyst were employed in the flask with stirring. The reaction mixture was monitored by using a gas chromatograph with a flame ionization detector. The recycled catalyst is also tested for the same reaction.

3. Results and Discussion

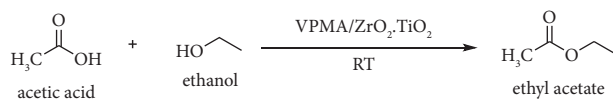
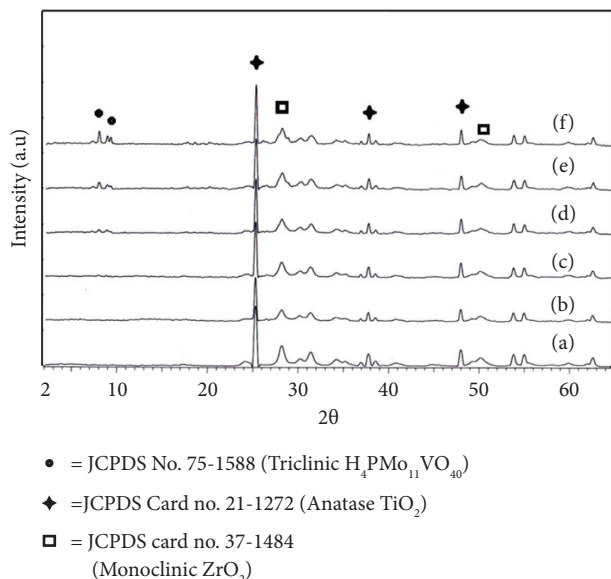
The X-ray diffraction patterns of various wt% of VPMA on $ZrO_2.TiO_2$ catalysts are shown in Figure 1. It can be seen from the XRD profile which exhibits the characteristic monoclinic phase (JCPDS card no. 37–1484) of ZrO_2 [24] at $2\theta = 28^\circ$ and 50° , JCPDS card no. 21–1272 anatase phase of TiO_2 [25] at $2\theta = 25^\circ$, 38° , and 48° . In contrast, VPMA's Keggin ion is located between $2\theta = 8.1^\circ$ and 9.5° [3]. Additionally, it is clear from JCPDS no. 75–1588 [26] of triclinic $H_3PMo_{12}O_{40}$ (Keggin ion structure) that vanadium is successfully introduced and maintains Keggin ion structure after vanadium incorporation into phosphomolybdic acid. This result suggests that vanadium is preserved during catalyst formation. [3]. [26] As the active phase of VMPA loading increased from 10 to 50 wt% on $ZrO_2.TiO_2$ mixed oxide support, crystallites of Keggin ion units were observed at higher loadings than lower loadings. Therefore, the active phase of VPMA is highly dispersed at lower loadings, and crystalline or bulk nature of Keggin ion is observed at higher VPMA loadings.

The Keggin ion density of VPMA/ $ZrO_2.TiO_2$ catalysts was calculated by the following equation:

$$\text{Keggin anion density (nm}^{-2}\text{)} = \frac{\text{HPA loading (wt \% / 100)} \times 6.02 \times 10^{23} \text{ (mol}^{-1}\text{)}}{\text{BET surface area (nm}^2\text{/g)} \times \text{FWHPA (g/mol)}} \quad (1)$$

The Keggin ion density results provide the information about the number of Keggin anions per square nanometer of the zirconia and titania mixed oxide surface. It is calculated according to the active phase VPMA loading and the catalyst surface area. Subsequently, each Keggin cluster (KU)

occupies around 1.44 nm^2 [5] and the theoretical monolayer of KU with 0.69 KU nm^{-2} is formed. The Keggin ion densities of synthesized samples are in the range of 0.28 to 2.25 which shows that ~20 VPMA/ $ZrO_2.TiO_2$ catalysts are well below the theoretical monolayer coverage (0.69 HPA/nm^2).

SCHEME 1: Synthesis of ethyl acetate from acetic acid and ethanol over VPMA/ZrO₂·TiO₂ catalysts.FIGURE 1: X-ray diffraction patterns of various wt% of VPMA/ZrO₂·TiO₂ catalysts (a) pure ZrO₂·TiO₂ (b) 10 (c) 20 (d) 30 (e) 40 (f) 50.

These findings indicate that the VPMA is highly dispersed over support surface at lower active phase loadings than higher loadings. This is due to covering and plugging of pores by the large Keggin ion leads to decrease in the surface area of the catalysts. Thus, the BET results (Table 1) are suggesting that at lower active phase loadings, the active phase Keggin ion density is well below the theoretical monolayer and is highly dispersed on the support. This result clearly demonstrates that at 50 wt% loading, the BET surface area is significantly reduced than other loadings which provide bulk formation of VPMA observed at higher loadings.

The acidity, BET surface area, and Keggin ion density results are tabulated in Table 1, and ammonia TPD profile is shown in Figure 2. These acidity measurements reveal that acidity values are inclined from 10 to 40 wt % of VPMA and minimized at 50 wt% loading. The BET surface area results provide information about the surface area which is significantly minimized at higher VPMA loadings, and this finding well correlates with Keggin ion density observed with respect to active phase loadings. Thus, acidity is declined at higher loading which is due to the bulk formation of VPMA on support, leading to the blockage of the pores of the support. This result number available acidic site was minimized at higher loading.

To investigate the nature of acidic sites by pyridine, adsorbed samples were recorded on the FT-IR spectrometer (Figure 3). The various wt% of VPMA on ZrO₂·TiO₂ catalysts exhibits 3 characteristic IR bands at 1532–1535, 1482–1485, and 1442–1443 cm⁻¹ that were attributed to

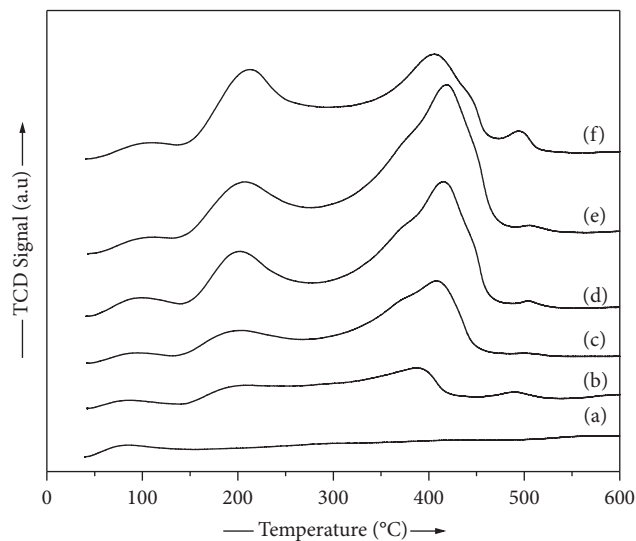
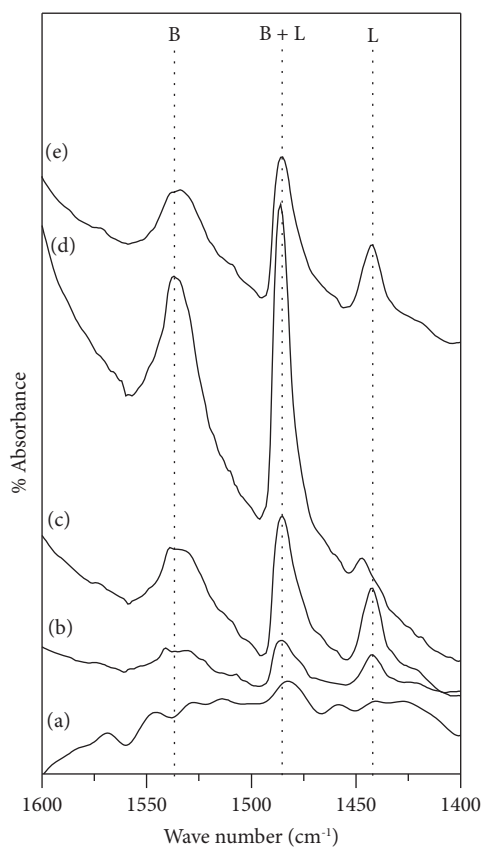
Brønsted (B), Brønsted + Lewis (B + L), and Lewis (L) acidic sites, respectively. This finding reveals that higher amount of Brønsted acidic sites than Lewis acidic sites were observed at higher loadings than lower loadings.

The morphology of catalysts is analyzed and is shown in Figure 4. These findings indicate pure VPMA which shows cylindrical morphology, whereas 20 wt% active phase loadings on support were evenly distributed, and at 40 wt%, it shows small crystallites of VPMA observed on support. However, at 50 wt%, loading on support reveals bulk or larger crystallites that were observed during SEM analysis. This SEM analysis well correlates with XRD finding as well as BET surface area of the catalysts.

Initially, the blank and catalytic reaction is performed for the esterification of acetic acid with ethanol, and results are tabulated in Table 2. The blank reaction without catalyst produces 1.5% yield of ethyl acetate. Whereas, VPMA catalyst exhibits 58% yield towards ethyl acetate. In the case of various VPMA loadings on mixed oxide support, 40 wt % VPMA loading behaves higher yield 93% of ethyl acetate than other loadings. These results were strongly inclined with acidity, amount, and number of Brønsted and Lewis acidic sites (Figure 3) of the catalysts as well as the surface area and Keggin ion density of the catalysts. The higher amount of acidity/more number of B & L acidic sites of the catalysts favours the better catalytic yield of ethyl acetate. This is in turn of lower crystallinity which was observed at lower VPMA loading than higher loadings correlates with BET surface area of the catalyst as well as SEM analysis. Therefore, at 40 wt% loading behaves more number of

TABLE 1: BET surface area, Keggin ion density, and acidity of VPMA/ZrO₂.TiO₂ catalysts.

Catalyst	BET surface area (m ² /g)	Keggin ion density (HPA/nm ²)	Acidity (mmol/g)
ZrO ₂ .TiO ₂	120	—	0.05
VPMA	7.5	4.5	2.4
10	119	0.28	0.9
20	115	0.58	2.3
30	103	0.98	3.4
40	98	1.38	4.5
50	75	2.25	3.1

FIGURE 2: Ammonia-TPD profile of various wt% of VPMA/ZrO₂.TiO₂ catalysts: (a) pure ZrO₂.TiO₂, (b) 10, (c) 20, (d) 30, (e) 40, and (f) 50.FIGURE 3: Pyridine adsorbed FT-IR spectra of various wt% of VPMA/ZrO₂.TiO₂ catalysts: (a) 10, (b) 20, (c) 30, (d) 40, and (e) 50.

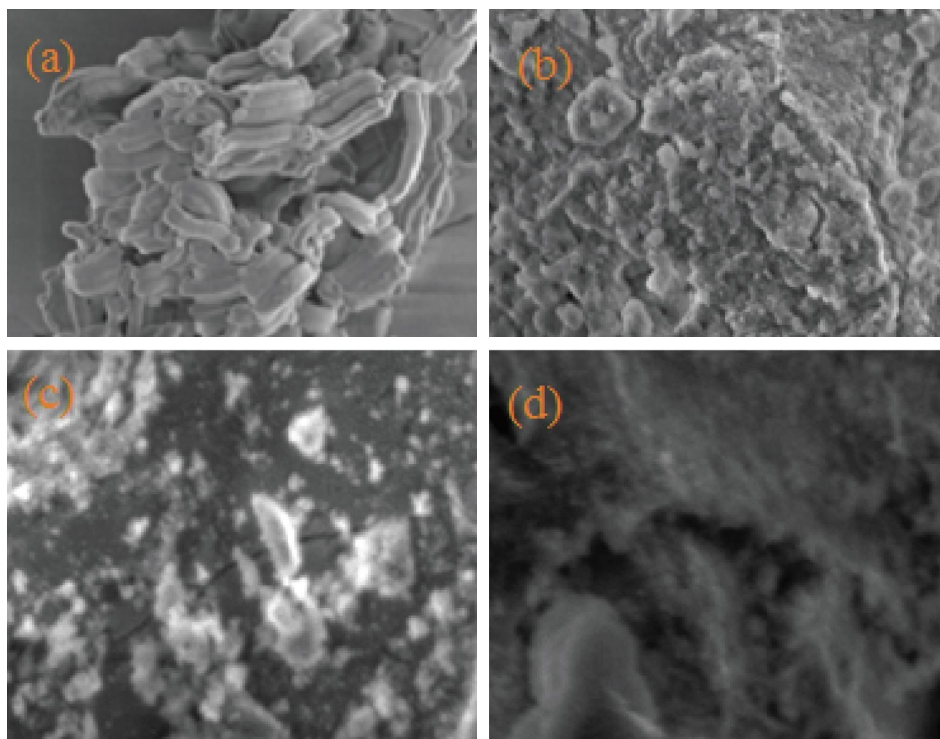


FIGURE 4: SEM analysis of various wt% of VPMA/ZrO₂.TiO₂ catalysts: (a) VPMA, (b) 20, (c) 40, and (d) 50.

TABLE 2: Catalytic results over VPMA/ZrO₂.TiO₂ catalysts^a.

Catalysts	Conversion (%)	Ethyl acetate yield (%)
Blank	1.5	1.5
VMPA	58	58
10	42	42
20	68	68
30	83	83
40	93	93
50	76	76

^aReaction conditions: 10 mmol (acetic acid), 20 mmol (ethanol), catalyst = 0.1 g, room temperature.

Brønsted as well as Lewis acidic sites (Figure 3) than other loadings, boasting the acetic acid conversion towards ester formation during the course of reaction.

The effect of mole ratio of acetic acid to ethanol was performed over 40 wt% VPMA/ZrO₂.TiO₂ catalyst (Table 3). These results indicated that ester yield increased from 78 to 93% with an increase in the mole ratio of acetic acid to ethanol from 1:1 to 1:2, respectively. Whereas, higher amount of ethanol used during course of reaction results drop in the ethyl acetate formation is due to further dilution of acetic acid noticeably.

The effect of catalytic amount of 40 wt% VPMA/ZrO₂.TiO₂ catalysts was tested, and results are tabulated in Table 4. It can be seen from Table 4, the ethyl acetate formation increases from 68% to 93% when catalytic amount of 0.05 g changes to 0.1 g, respectively. However, there is no significant change in ethyl acetate when higher amount of catalyst is used.

TABLE 3: Catalytic results of various mole ratios of reactants over the 40 wt% VPMA/ZrO₂.TiO₂ catalyst^a.

Mole ratio (acetic acid/ethanol)	Acetic acid conversion (%)	Ethyl acetate yield (%)
1 : 1	78	78
1 : 2	93	93
1 : 3	75	75
1 : 4	69	69
1 : 8	67	67

^aReaction conditions: 10 mmol (acetic acid), 10–80 mmol (ethanol), catalyst = 0.1 g, room temperature.

TABLE 4: Catalytic results of various amounts of 40 wt% VPMA/ZrO₂.TiO₂ catalysts^a.

Catalyst amount (g)	Acetic acid conversion (%)	Ethyl acetate yield (%)
0.05	68	68
0.1	93	93
0.2	94	94
0.3	95	95

^aReaction conditions: 10 mmol (acetic acid), 20 mmol (ethanol), catalyst = 0.05–0.3 g, room temperature.

The formation of yield of ethyl acetate with respect to reaction time is monitored over 40 wt% of VPMA on mixed oxide support, and results are tabulated in Table 5. The time on stream analysis indicated that increase in the conversion with time reaches maximum 95% ethyl acetate yield at 36 h at room temperature, and further reaction time equilibrium yield is maintained.

TABLE 5: Catalytic results of TOS over 40 wt% VPMA/ZrO₂.TiO₂ catalyst^a.

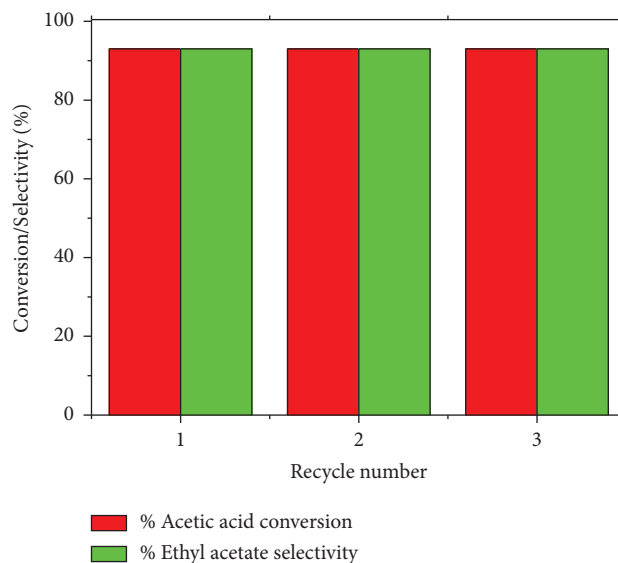
Reaction time (h)	Acetic acid conversion (%)	Ethyl acetate yield (%)
4	26	26
8	48	48
12	59	59
16	76	76
20	85	85
24	93	93
30	94	94
36	95	95
42	95	95
48	95	95
52	95	95

^aReaction conditions: 10 mmol (acetic acid), 20 mmol (ethanol), catalyst = 0.1 g, room temperature.

TABLE 6: Catalytic results of esterification with various alcohols over 40 wt% VPMA/ZrO₂.TiO₂ catalysts^a.

Alcohol	Acetic acid conversion (%)	Ester yield (%)
Methanol	96	96
Ethanol	93	93
Butanol	79	79
Hexanol	62	62
Benzyl alcohol	83	83

^aReaction conditions 10 mmol (acetic acid), 20 mmol (alcohol), catalyst = 0.1 g, room temperature.

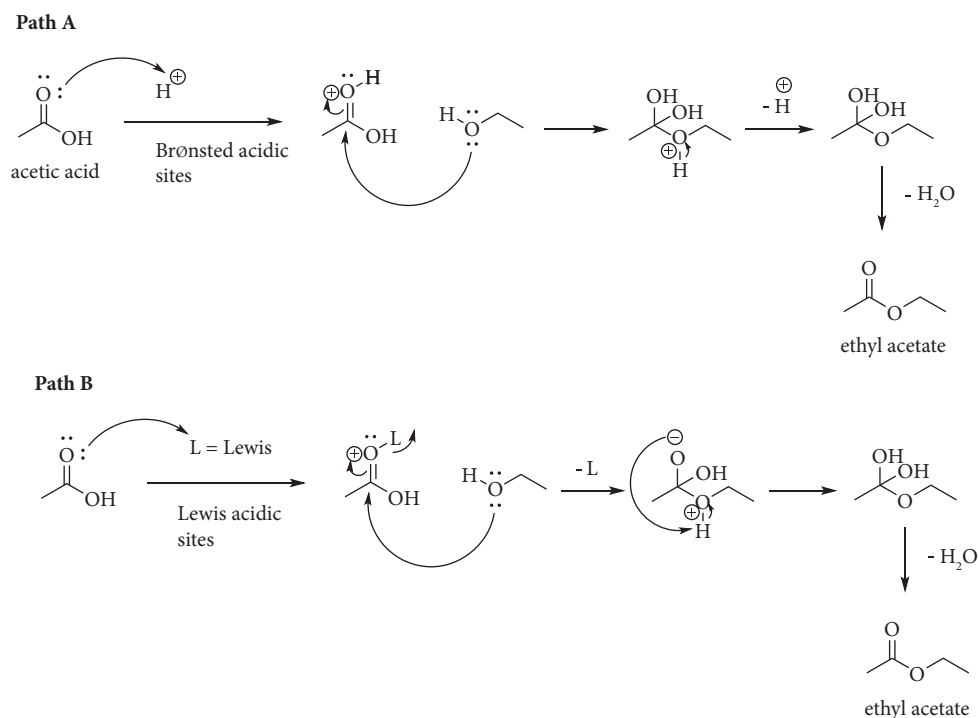
FIGURE 5: Recycle studies over 40 wt% VPMA/ZrO₂.TiO₂ catalyst.

The catalytic performance of acetic acid with various alcohols was studied at the same reaction conditions, and the results are tabulated in Table 6. These findings reveal that formation of ester is declined with increase of carbon chain of the alcohol. Therefore, methanol produced higher yield than other alcohols used during the reaction.

The catalyst stability during reaction was examined by the recycling experiment which is shown in Figure 5. Before going to perform recycling, after the reaction catalyst and reaction mixture were centrifuged and then separated and dried in an oven at 100°C which were

thereafter calcined at 200°C for 3 h in air. Now, the regenerated catalyst was tested for the same reaction. The catalytic conversion reveals that the catalyst exhibits stable activity during the 3 cycles of reactions (Figure 5). Thus, the catalyst shows stable conversion or yield during regeneration studies.

3.1. Reaction Mechanism. In order to find the formation, esters form acetic acid and ethanol through mechanism over Brønsted and Lewis acidic sites which is shown in Scheme 2. Ethyl acetate was produced via two pathways, and those are

SCHEME 2: Mechanism over Brønsted and Lewis acidic sites of VPMA/ZrO₂.TiO₂ catalyst.TABLE 7: Comparison study of various catalysts with VPMA/ZrO₂.TiO₂ catalyst for esterification of acetic acid.

Catalysts	Surface area (m ² /g)	Reaction temperature (°C)	Ethyl acetate yield (%)	Ref.
HPW/kaolinite	9	90	75	[27]
AEI-type zeolite membrane	—	90	84	[28]
20 wt% DPTA/K10	135	100	89.8	[29]
30 wt% DPTA/K10	104	100	90	[29]
40 wt% VPMA/ZrO ₂ .TiO ₂	98	Room temperature	93	Present work

path A and path B, respectively. In path A, Brønsted acidic sites or protons making coordination with a lone pair of oxygen in carbonyl group makes carbonyl carbon which is more electron-deficient. After that, a lone pair on oxygen in alcohol is attacked on electron-deficient carbonyl carbon that leads to loss of water molecule to produce ethyl acetate. In path B, similar to path A, the Lewis (L) acidic sites pull the carbonyl carbon more electron-deficient and attack of lone pair on oxygen in alcohol at carbonyl carbon favours the formation of ethyl acetate.

The comparison of the present study with literature of acetic acid esterification over various catalysts is shown in Table 7. Alsalmeh et al. [27] studied the esterification of acetic acid with ethanol at 90°C to produce 75% yield of ester. Whereas, Sekine et al. [28] carried out esterification of acetic acid over AEI-type zeolite membrane at 90°C to produce 84% yield. Gurav et al. [29] reported acetic acid esterification in the presence of 20 and 30 wt% DPTA/K10 at 100°C, showing 89.8 and 90% ethyl acetate yields, respectively. However, in the present study, 40 wt% VPMA/ZrO₂.TiO₂ exhibits 93% yield towards ethyl acetate at room temperature. The VPMA/ZrO₂.TiO₂ catalyst provides better catalytic

yield than other catalysts even when the reaction operated at room temperature.

4. Conclusions

Vanadium boosted the phosphomolybdic acid catalyst supported on ZrO₂.TiO₂ oxide-supported catalysts which efficiently conducted selective esterification of acetic acid to ethyl acetate at room temperature. 40 wt% VPMA/ZrO₂.TiO₂ catalyst exhibits higher catalytic performance during the course of reaction than other VPMA loadings. The catalytic functionality well reveals with structural and acidic properties of the catalyst. The XRD finding clearly indicated that the active phase of VPMA is highly dispersed at lower loadings as well as crystallites of Keggin ion are observed at higher loadings. TPD of ammonia data reveals that acidity is inclined with VPMA loading on support. BET surface area analysis shows that a higher surface area of the catalyst provides lower Keggin ion density. SEM images clearly illustrated that bulk formation of VPMA on support was observed at higher loadings. Pyridine-adsorbed FT-IR spectra suggest that Brønsted and Lewis acids favour the formation of ethyl acetate

during the reaction. The recycle studies show stable catalytic functionality up to 3 cycles during the reaction.

Data Availability

The data that support the findings of this study are included in this article.

Conflicts of Interest

The author declares that there are no conflicts of interest.

Acknowledgments

The author thanks to the GMR Institute of Technology, Rajam.

References

- [1] I. V. Kozhevnikov, "Catalysis by heteropoly acids and multicomponent polyoxometalates in liquid-phase reactions," *Chemistry Review*, vol. 98, no. 1, pp. 171–198, 1998.
- [2] N. Mizuno and M. Misono, "Heterogeneous catalysis," *Chemistry Review*, vol. 98, no. 1, pp. 199–218, 1998.
- [3] B. Viswanadham, P. Jhansi, K. V. R. Chary, H. B. Friedrich, and S. Singh, "Efficient solvent free knoevenagel condensation over vanadium containing heteropolyacid catalysts," *Catalysis Letters*, vol. 146, no. 2, pp. 364–372, 2016.
- [4] B. Viswanadham, J. Pedada, H. B. Friedrich, and S. Singh, "The role of copper exchanged phosphomolybdic acid catalyst for knoevenagel condensation," *Catalysis Letters*, vol. 146, no. 8, pp. 1470–1477, 2016.
- [5] B. Viswanadham, V. Pavankumar, and K. V. R. Chary, "Vapor phase dehydration of glycerol to acrolein over phosphotungstic acid catalyst supported on niobia," *Catalysis Letters*, vol. 144, no. 4, pp. 744–755, 2014.
- [6] B. Viswanadham, A. Srikanth, and K. V. R. Chary, "Characterization and reactivity of 11-molybdo-1-vanadophosphoric acid catalyst supported on zirconia for dehydration of glycerol to acrolein," *Journal of Chemical Sciences*, vol. 126, no. 2, pp. 445–454, 2014.
- [7] B. Viswanadham, A. Srikanth, V. P. Kumar, and K. V. R. Chary, "Vapor phase dehydration of glycerol to acrolein over SBA-15 supported vanadium substituted phosphomolybdic acid catalyst," *Journal of Nanoscience and Nanotechnology*, vol. 15, no. 7, pp. 5391–5402, 2015.
- [8] B. Viswanadham, V. Vishwanathan, K. V. R. Chary, and Y. Satyanarayana, "Catalytic dehydration of glycerol to acrolein over mesoporous MCM-41 supported heteropolyacid catalysts," *Journal of Porous Materials*, vol. 28, no. 4, pp. 1269–1279, 2021.
- [9] B. Viswanadham and K. V. R. Chary, "Eco-friendly vapor phase aerobic selective oxidation of styrene to benzaldehyde over SBA-15 supported vanadium modified heteropolyacid catalyst," *Catalysis Letters*, vol. 152, no. 11, pp. 3447–3452, 2022.
- [10] S. Yamaguchi, S. Sumimoto, Y. Ichihashi, S. Nishiyama, and S. Tsuruya, "Liquid-phase oxidation of benzene to phenol over V-substituted heteropolyacid catalysts," *Industrial & Engineering Chemistry Research*, vol. 44, pp. 1–7, 2005.
- [11] G. Wang, Y. Han, F. Wang, Y. Chu, and X. Chen, "Catalytic oxidative desulfurization of benzothiophene using silica-supported heteropolyacid catalyst: activity, deactivation and regeneration of the catalyst," *Reaction Kinetics, Mechanisms and Catalysis*, vol. 115, no. 2, pp. 679–690, 2015.
- [12] L. Marosi, G. Cox, A. Tenten, and H. Hibst, "In situ XRD investigations of heteropolyacid catalysts in the methacrolein to methacrylic acid oxidation reaction: structural changes during the activation/deactivation process," *Journal of Catalysis*, vol. 194, no. 1, pp. 140–145, 2000.
- [13] Z. Long, Y. Zhou, G. Chen, W. Ge, and J. Wang, " C_3N_4 - $H_5PMo_{10}V_2O_{40}$: a dual-catalysis system for reductant-free aerobic oxidation of benzene to phenol," *Scientific Reports*, vol. 4, no. 1, p. 3651, 2014.
- [14] F. Zhang, M. Guo, H. Ge, and J. Wang, "Hydroxylation of benzene with hydrogen peroxide over highly efficient molybdovanadophosphoric heteropoly acid catalysts," *Chinese Journal of Chemical Engineering*, vol. 15, no. 6, pp. 895–898, 2007.
- [15] P. Sharma and A. Patel, "Liquid phase non-solvent selective oxidation of styrene using aqueous hydrogen peroxide with supported 12-tungstophosphoric acid," *Indian Journal of Chemistry*, vol. 48, pp. 964–968, 2009.
- [16] I. K. Song, J. K. Lee, G. I. Park, and W. Y. Lee, "Selective oxidation catalysis over heteropoly acid supported on polymer," *Studies in Surface Science and Catalysis*, vol. 110, pp. 1183–1192, 1997.
- [17] M. Misono, "Unique acid catalysis of heteropoly compounds (heteropolyoxometalates) in the solid state," *Chemical Communications*, vol. 13, pp. 1141–1152, 2001.
- [18] B. M. Reddy and A. Khan, "Recent advances on TiO_2 - ZrO_2 mixed oxides as catalysts and catalyst supports," *ChemInform*, vol. 36, no. 40, pp. 257–296, 2005.
- [19] Z. Xi, W. Jia, and Z. Zhu, " WO_3 - ZrO_2 - TiO_2 composite oxide supported Pt as an efficient catalyst for continuous hydrogenolysis of glycerol," *Catalysis Letters*, vol. 151, no. 1, pp. 124–137, 2021.
- [20] S. K. Maity, M. S. Rana, S. K. Bej, J. Ancheyta-Juárez, G. Murali Dhar, and T. Prasada Rao, " TiO_2 - ZrO_2 mixed oxide as a support for hydrotreating catalyst," *Catalysis Letters*, vol. 72, no. 1/2, pp. 115–119, 2001.
- [21] J. Cao, B. Qi, J. Liu et al., "Deep eutectic solvent choline chloride-2CrCl₃·6H₂O: an efficient catalyst for esterification of formic and acetic acid at room temperature," *RSC Advances*, vol. 6, no. 26, pp. 21612–21616, 2016.
- [22] L. Gang, L. Xinzong, and W. Eli, "Solvent-free esterification catalyzed by surfactant-combined catalysts at room temperature," *New Journal of Chemistry*, vol. 31, no. 3, pp. 348–351, 2007.
- [23] D. Jiang, Y. Y. Wang, and L. Y. Dai, "Esterification of alcohols with acetic anhydride in Brønsted acidic ionic liquids at room temperature," *Reaction Kinetics and Catalysis Letters*, vol. 93, no. 2, pp. 257–263, 2008.
- [24] S. Limbu, "Investigation of crystal structure confinement and optical attributes of monoclinic-tetragonal Zirconia nanocrystals via chemical co-precipitation technique," *Bulletin of Materials Science*, vol. 45, no. 4, p. 182, 2022.
- [25] W. Li, R. Liang, A. Hu, Z. Huang, and Y. N. Zhou, "Generation of oxygen vacancies in visible light activated one-dimensional iodine TiO_2 photocatalysts," *RSC Advances*, vol. 4, no. 70, pp. 36959–36966, 2014.
- [26] H. Zhang, C. Yang, S. Zhao, T. Wang, and W. Zhu, "Comparison in thermal stability and catalytic performance of $H_4PMo_{11}VO_{40}$ heteropolyacid supported on mesoporous and macroporous silica materials," *Journal of Chemical Research*, vol. 45, no. 1-2, pp. 60–67, 2020.
- [27] A. Alsalmeh, A. A. Alsharif, and H. A. Enizi, "Probing the catalytic efficiency of supported heteropoly acids for

esterification: effect of weak catalyst support interactions,” *Journal of Chemistry*, vol. 2018, Article ID 7037461, 10 pages, 2018.

- [28] Y. Sekine, M. Sakai, and M. Matsukata, “Esterification of acetic acid by flow-type membrane reactor with AEI zeolite membrane,” *Membranes*, vol. 13, no. 1, p. 111, 2023.
- [29] H. Gurav and V. V. Bokade, “Synthesis of ethyl acetate by esterification of acetic acid with ethanol over a heteropolyacid on montmorillonite K10,” *Journal of Natural Gas Chemistry*, vol. 19, no. 2, pp. 161–164, 2010.